Spontaneous Gradients by ATRP and RAFT: Interchangeable Polymerization Methods?

Kate G E Bradford, Robert D Gilbert, M. A. Sachini, M. Weerasinghe, Simon Harrisson, Dominik Konkolewicz

Spontaneous Gradients by ATRP and RAFT: Interchangeable Polymerization Methods?

Kate G. E. Bradford,[a†] Robert D. Gilbert,[a†] M. A. Sachini N. Weerasinghe,[a] Simon Harrisson,[b] Dominik Konkolewicz [a*]

a Department of Chemistry and Biochemistry, Miami University, 651 E High St, Oxford, OH, USA
b Laboratoire de Chimie des Polymères Organiques, University of Bordeaux/Bordeaux INP/CNRS UMR5629, Pessac 33600, France
† Authors contributed equally
*Correspondence: d.konkolewicz@miamiOH.edu

Abstract

The spontaneous gradient polymerization was, herein, investigated by ATRP and RAFT. The model monomers for both systems were methyl methacrylate (MMA) and ethyl acrylate (EA). Spontaneous gradient polymers were generated, however, the control over polymer structure varied with both the polymerization method and initiator structure. RAFT polymerization was found to have the best control while using a chain transfer agent (CTA) compatible with both the methacrylic and acrylic monomers. The use of this dual compatible CTA allowed for the RAFT polymerization gave excellent correlation of experimental and theoretical molecular weight, dispersities below 1.3, and reactivity ratios consistent with spontaneous gradient formation. In contrast, the RAFT CTA with a less effective homolytic leaving group led to poor correlation between experimental and theoretical molecular weights, and dispersity typically above 1.5. In general, ATRP led to somewhat higher dispersity polymers in the order of 1.4-1.5 with decreased correlation of experimental and theoretical molecular weights, despite the formation of gradients. Reactivity ratios for both MMA and EA were determined using a terminal reactivity model. The reactivity ratios were similar to those in conventional radical polymerization, as the propagating radicals are identical. Although similar, RAFT and ATRP are not fully interchangeable in gradient polymerization, with RAFT offering a simpler approach to gradient polymers when a CTA compatible with both monomers is selected.

Introduction

Polymer architecture is an important parameter that controls material properties and can introduce new functions to the polymers.[1–4] In addition to the classical linear homopolymer, there are many types of complex polymer architectures including star, brush, hyperbranched, dendritic, as well as complex copolymers such as block and gradient copolymers.[3,5–7] Gradient polymers have a gradual drift in polymer composition from being rich in one monomer near the alpha terminus, transitioning to rich in a second monomer near the omega terminus.[8–11] Gradient polymers offer unique properties[12–14] such as broad T_g ranges,[15–17] responsive self-assembly,[18,19] perturbation of polymer pKa,[20] "reel-in" micelles,[21,22] and they can also serve as compatibilizers for polymer blends.[23–26] Due to these unique functionalities and properties, it is important to design new methods of gradient polymer synthesis, understand differences in polymerization methods, and also to evaluate the properties of the synthesized gradients.[3,5,8,27]

In general, gradient polymers are synthesized by living or reversible deactivation processes, as these methods ensure the majority of chains continue to grow through the reaction where the monomer composition changes.[3,5,7–9,28–32] Integral to most gradient polymer syntheses is a compositional drift over the course of the reaction. This compositional change can be achieved either by using monomers with dramatically different reactivity,[13,15,19,33–35] or by changing the feed of monomers over the course of the reaction.[18,32,36–44] The first approach, known as the intrinsic or spontaneous gradient approach, relies on choosing monomers such that one monomer is preferentially incorporated at the start of the reaction, leaving an excess of the second monomer to be incorporated at the later stages of the reaction.[32,45] In the second type of system, known as a forced or extrinsic gradient polymer, careful design of monomer feeds need to be performed to ensure the gradient structure is obtained,[18,41] rather than a block-like or statistical polymer.

However, forced gradient approaches can, in principle, be applied to any monomer pairs that readily copolymerize.[32,45] In contrast, the spontaneous gradient approach is simpler to set up as it requires no feed of the two monomers, but it is limited to monomers with substantially different reactivities.

The reversible deactivation radical polymerization methods of reversible addition-fragmentation chain transfer (RAFT) and atom transfer radical polymerization (ATRP) are well-adapted for gradient copolymer synthesis.[30] This due to the fact that both RAFT and ATRP are compatible with a wide range of monomers and use mild reaction conditions to produce polymers of predictable molecular weight, relatively narrow dispersity, and high chain-end functionality. In many cases, choosing either RAFT or ATRP methodologies can be used to synthesize well-controlled polymers,[30] although, in certain cases such as network formation, one method can give better defined polymers.[46] Several studies have harnessed the use of monomer reactivity to create spontaneous and forced gradient copolymers by ATRP as well as forced gradient copolymers[14,41–44,47,48] by RAFT.[18,37,39,40] There are fewer reports on spontaneous RAFT gradient copolymers,[13,15,19,33–35] although the gradient properties of other methacrylic/acrylic copolymers prepared by RAFT have been discussed but lack a detailed kinetic analysis.[49–54] However, to the best of our knowledge, no systematic analysis comparing spontaneous gradient copolymers by RAFT and ATRP have yet been performed. This analysis of polymers made under similar conditions by both RAFT and ATRP such that they can be used to critically evaluate the processes, highlight their similarities and differences, and ultimately determine the optimal conditions for the preparation of well-controlled gradient polymers.

Kinetic Framework and Model Systems

The mechanisms of ATRP and RAFT polymerizations are shown in Schemes 1A and 1B, respectively, with radical generation from a conventional initiator given in Scheme 1C. In ATRP, the Cu^{I}/L activator abstracts the halogen from the chain end, which in this system could be MMA or EA, with rate coefficient k_{act}.[55] This generates the oxidized Br-Cu^{II}/L deactivator complex and a propagating radical. The radical is then able to add monomer, terminate with rate coefficient k_t, or be deactivated by the Br-Cu^{II}/L complex with rate coefficient k_{deact}, returning the chain to the dormant state and reforming the Cu^{I}/L activator complex.[55] In ARGET ATRP, a reducing agent, such as ascorbic acid, is added to prevent the build-up of excess Br-Cu^{II}/L due to the unavoidable termination of radicals.[56] This reduces Br-Cu^{II}/L with rate coefficient k_{red}.[57–59] The RAFT process occurs through a degenerate equilibrium, facilitated by an addition-fragmentation sequence.[60,61] Similarly to ATRP, the terminal units of the propagating radical and chain transfer agent (CTA) can be MMA or EA. A propagating radical adds to the thiocarbonylthio group of the CTA, with rate coefficient k_{add}, generating the RAFT intermediate radical.[61,62] The RAFT intermediate subsequently fragments, with rate coefficient k_{frag}, releasing either the original propagating radical and reforming the original CTA, or transferring the thiocarbonylthio group to the chain that was originally a propagating radical and simultaneously generating a new propagating radical.[30] Due to the termination processes intrinsic to radical polymerization, radicals must constantly be supplied from an initiator, I-I, which decomposes with rate coefficient k_d.[61] These initiator fragment radicals can subsequently add either MMA or EA monomer, generating new propagating radicals.[30,61]

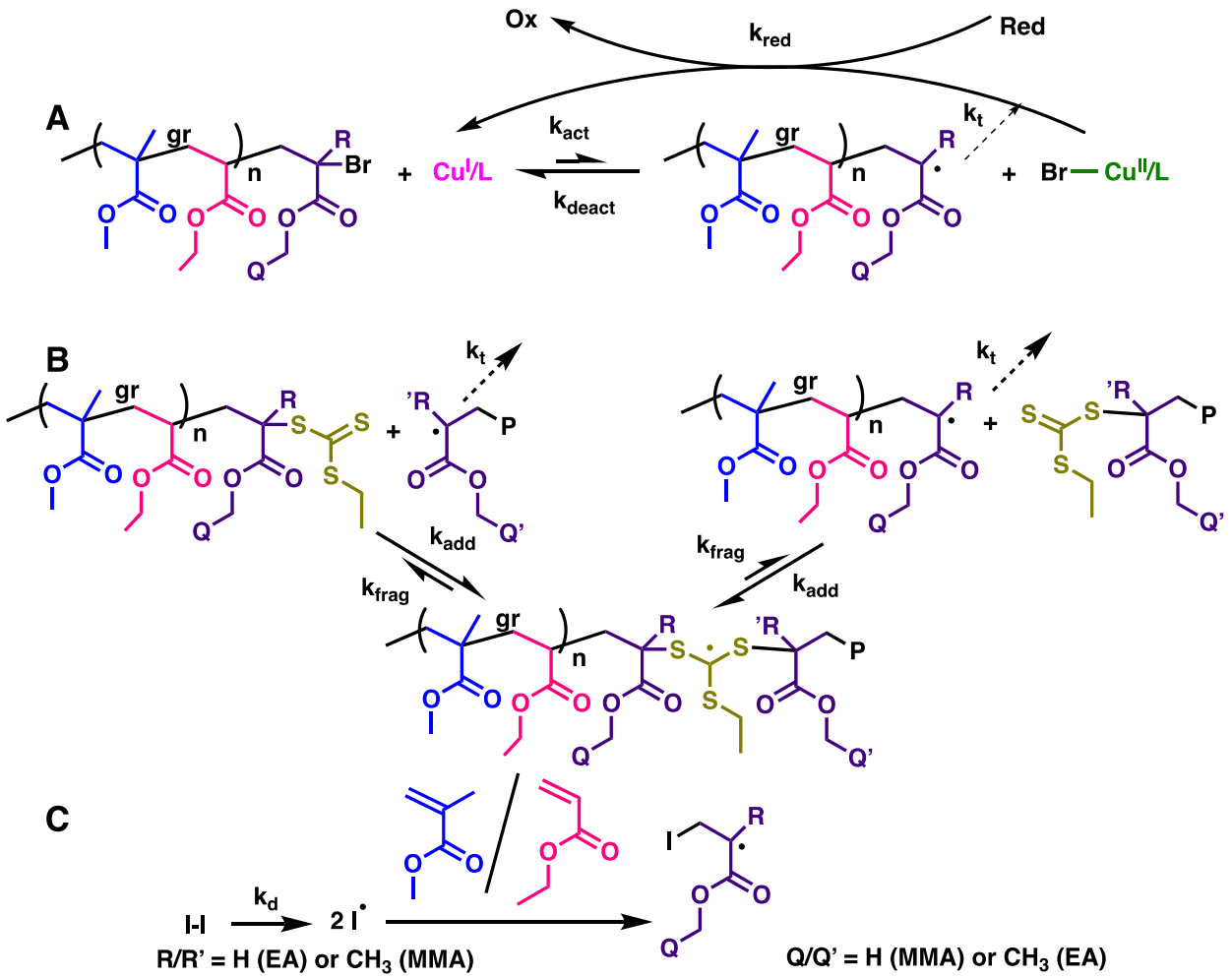

Scheme 1: A) Mechanism of ARGET ATRP activation and deactivation in the main ATRP equilibrium B) Mechanism of RAFT degenerative exchange in the RAFT main equilibrium. C) Propagating radical generation in RAFT by dissociation of a thermal initiator (I-I).

When considering propagation in radical copolymerization of two monomers, the simplest approach is to assume equal selectivity of the monomers to the distinct chain ends, giving an ideal copolymerization that can be described by a single kinetic parameter.[16] However, this approach is not typically valid for radical polymerizations, which frequently deviate from ideality. The terminal reactivity model is a more generally applicable model that captures the unequal selectivities of each chain end.[19,63–66] As shown in Scheme 2, this model supposes two distinct radical chain ends, one derived from addition of MMA, the other from addition of EA. Both the MMA- and EA-terminal chain ends can add either the MMA or EA monomer. This occurs with

rate coefficient $k_{X\text{-}Y}$, where X is the radical type and Y is the monomer to be added. From this the reactivity ratios $r_{MMA} = k_{MMA\text{-}MMA}/k_{MMA\text{-}EA}$ and $r_{EA} = k_{EA\text{-}EA}/k_{EA\text{-}MMA}$ can be given as the ratio of homopropagation to cross-propagation rate coefficients, as shown in Scheme 2.[63] The terminal model for copolymerization applies equally to ATRP and RAFT systems, since the propagating radicals are the same in both mechanisms.[30]

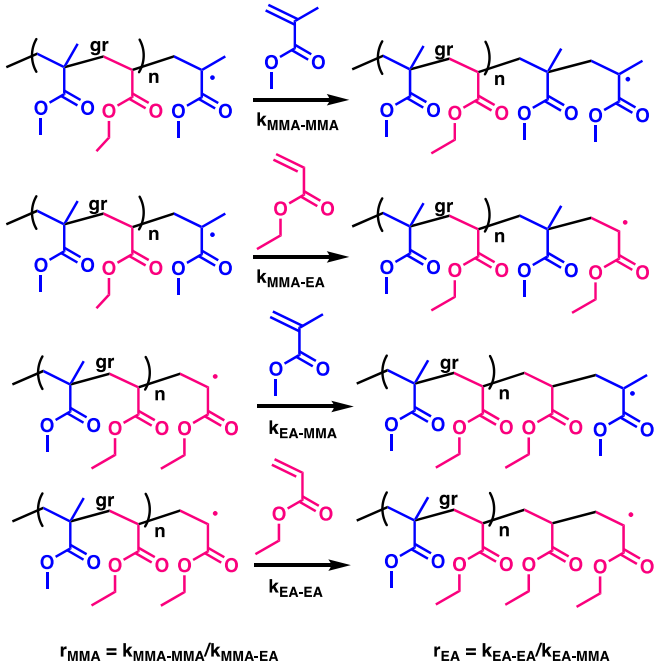

Scheme 2: Terminal model of copolymerization of MMA and EA, including derived reactivity ratios r_{MMA} and r_{EA}.

The systems used to compare the gradient copolymerization kinetics of ATRP and RAFT systems are shown in Scheme 3. Copolymerizations of MMA and EA were performed at 70 °C and analyzed using the terminal reactivity ratio model of Scheme 2. ATRP copolymerizations were carried out by an ARGET ATRP process with Cu/Me_6TREN as the catalyst (Scheme 3A). RAFT copolymerizations were carried out using thermal initiation by AIBN. One feature explored was the effect of the CTA's leaving group. Specifically, leaving groups were used that are well suited

for either the polymerization of both MMA and EA, or only EA. MMA forms a more stabilized tertiary propagating radical, while EA forms a less stabilized secondary propagating radical.

Due to the differences in stability of the radicals formed from incorporation of MMA and EA, these monomers have different reactivities, with faster incorporation of MMA than EA.[67] In ATRP, the two initiators were used were ethyl α-bromophenylacetate (EBPAc), which is among the most active ATRP initiators and well suited to MMA, and ethyl 2-bromopropionate (EBPr), which is less active and best suited to initiate EA[68]. Similarly in the case of RAFT, different homolytic leaving groups were used, although both CTAs had ethyltrithiocarbonate RAFT end groups. One RAFT agent, cyanoisopropyl ethyl trithiocarbonate (CPETC), contains the highly stabilized cyanoisopropyl leaving group,[69] which is well suited to both MMA and EA polymerization. The other is propionic acid ethyl trithiocarbonate (PAETC),[70] containing the less-stabilized 2-propionic acid-yl leaving group, which is well suited to EA polymerization. However, this secondary leaving group is insufficiently stabilized to fully convert to macroCTA at low conversion in the RAFT pre-equilibrium for MMA, making this CTA poorly suited for MMA polymerization.[61] In general for efficient ATRP and RAFT polymerization, the initiation rate should be substantially faster than or at least equal to the rate of monomer addition. Therefore, using a less active initiating fragment could adversely impact the control over the polymerization.

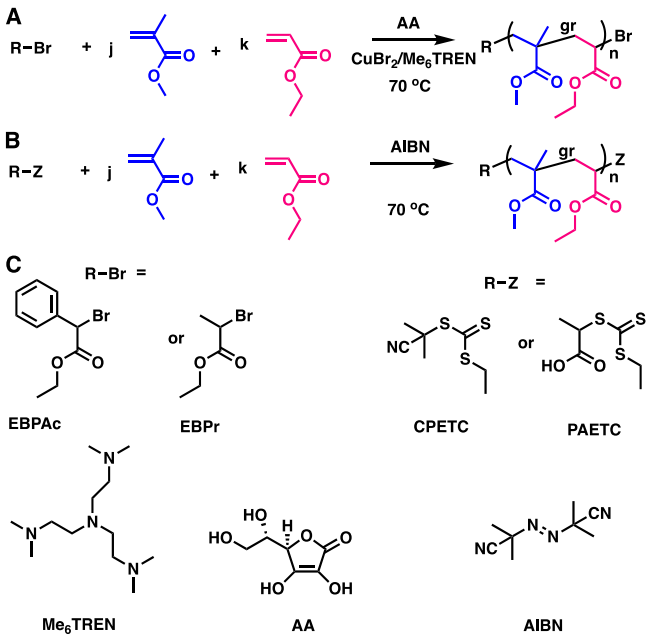

Scheme 3: A) Synthesis of gradient polymers of MMA and EA by ATRP. B) Synthesis of gradient polymers of MMA and EA by ATRP. C) Structures of ATRP initiators, RAFT CTAs, Me_6TREN ligand, ascorbic acid (AA) and AIBN.

Results and Discussion

Initially the ATRP copolymerization of MMA and EA was explored. Figure 1 shows the kinetics of the copolymerization MMA and EA, as well as the evolution of number averaged molecular weight (M_n) and dispersity (M_w/M_n) against the theoretical M_n ($M_{n\text{-th}}$). Figure 1 gives the kinetics and evolution using both the more active EBPAc and less active EBPr initiators. Figure 1A and 1B show the kinetics of MMA and EA consumption at target composition of MMA=EA=25 and MMA=EA=50 respectively. In general, close to linear first order kinetic plots are observed, and in all cases the MMA is consumed substantially faster than EA, suggesting a gradient like structure is generated. These data suggest that the rates of polymerization are only weakly affected by the choice of the initiator, EBPr vs EBPAc, which is especially prominent in Figure 1A, and consistent with the data in Figure 1B. The similarity of the rates after any initialization period is likely due to the initiator being consumed in the early phase of the reaction and converted to macroinitiator soon after the reaction commences.

Figure 1C indicates that the polymerizations had acceptable control over the reaction, with M_n increasing linearly with conversion and remaining close to the expected M_n, and dispersities in the order of 1.3-1.5. Despite the high catalyst loadings (1500 ppm for MMA25-EA25 and 1000 ppm for MMA50-EA50), M_n is measurably higher than $M_{n\text{-}th}$ and dispersities are in the order of 1.3-1.4 over the course of the reaction. As seen in Table S2, lower catalyst loadings led to even higher dispersity values and decreased control over the molecular weight of the polymer. This suggests that there are unique challenges in gradient ATRP polymerization, since catalyst loadings at or below 100 ppm have been successfully used in the homopolymerization of both methacrylates and acrylates.[57,59] In the ATRP systems of Figure 1C the more active EBPAc initiator appears to give similar molecular weights to the less active EBPr.

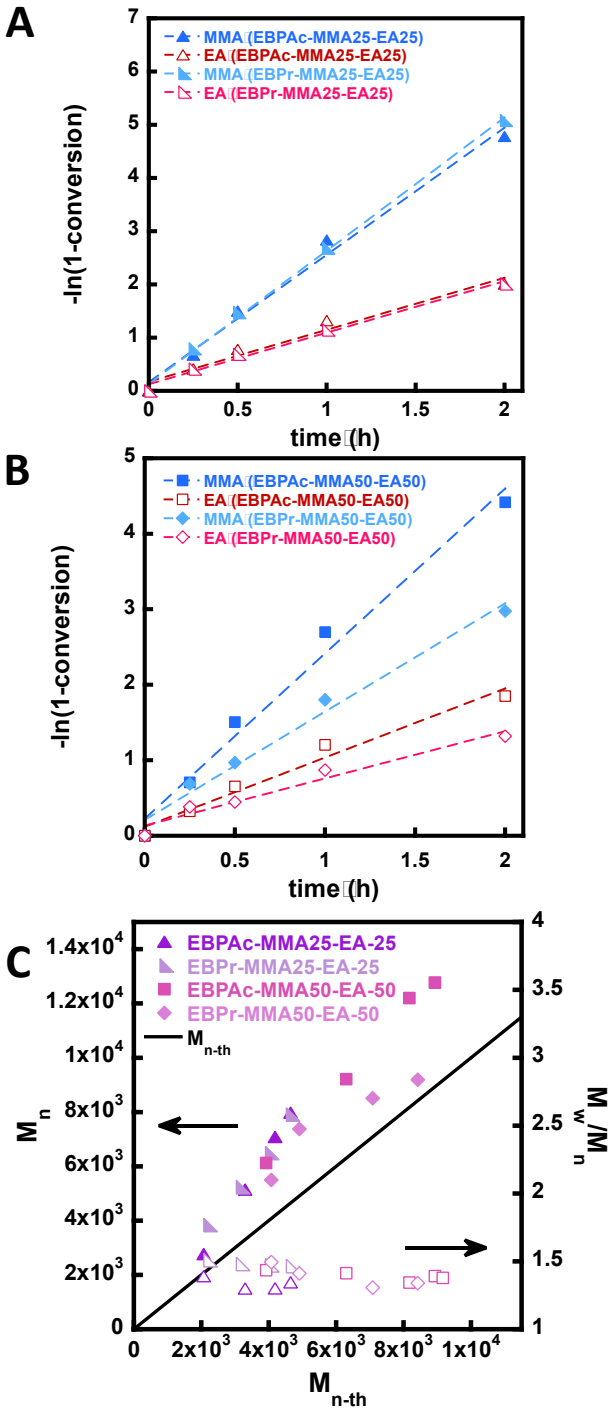

Figure 1: ARGET ATRP MMA-EA gradient polymers at different chain lengths. Conditions [MMA]:[EA]:[RBr]:[$CuBr_2$]:[Me_6TREN]:[AA]=50:50:1:0.1:0.6:0.2 or [MMA]:[EA]:[RBr]:[$CuBr_2$]:[Me_6TREN]:[AA]=25:25:1:0.075:0.45:0.2 in 50 vol % DMSO at 70 °C. RBr= EBPAc or EBPr A) Kinetics of polymerization at target chain length of 25 units of MMA and EA. B) Kinetics of polymerization at target chain length of 50 units of MMA and EA. C) Evolution of M_n and M_w/M_n with the $M_{n\text{-}th}$ evaluated from total monomer conversion.

Figure 2 highlights the influence of monomer ratio on the kinetics and control over polymerization. Three monomer feeds were considered, one rich in MMA; (MMA67-EA33), one even in both monomers; (MMA50-EA50), and one rich in EA; (MMA33-EA67). In all cases, the total chain length remained 100 monomer units. As seen in Figure 2A and 2B, higher ratios of the faster propagating EA monomer led to overall higher polymerization rates of both MMA and EA. In all cases, a gradient-like structure is generated with faster incorporation of MMA than of EA. These results broadly agree with the findings in Figure 1. Figure 2C and 2D show the correlation of M_n with $M_{n\text{-th}}$ and the evolution of dispersity with $M_{n\text{-th}}$.

In all cases, M_n increased linearly with $M_{n\text{-th}}$, although in most cases M_n was above $M_{n\text{-th}}$. This could be due to several factors and may be unique for each initiator. For EBPAc, it is possible that the highly active initiator could lead to some termination early in the reaction, causing the concentration of living ATRP macroinitiator to be lower than the initial concentration of EBPAc.[68] Conversely, the less active EBPr could have slightly lower activity than the acrylic and certainly the methacrylic chain ends. In this case, there could be a small fraction of unreacted EBPr, which causes the M_n to systematically exceed $M_{n\text{-th}}$. In general, all systems had similar dispersities in the order of 1.3-1.5, although higher concentrations of the less active EA monomer tended to give lower dispersities, which is shown in Figures 2C and 2D. This is most likely due to the more efficient deactivation of the acrylic radical which comprises a relatively larger amount of radical chain ends at higher EA loadings. Additionally, the faster addition of MMA to the EA-based radical chain end can increase the relative contribution of propagation compared to deactivation. This will lead to higher dispersity, since the ratio of propagation to deactivation is higher.[71–73] It is notable that the MMA/EA ATRP gradient copolymers using over 1000 ppm of Cu catalyst have dispersities approaching 1.5, the homopolymerizations of MMA and EA using ~100 ppm of catalyst tend to

have dispersities in the order of 1.1-1.3.[57,59] This difference could arise from challenges in deactivating both chain ends, faster incorporation of MMA to the acrylic radical chain end, and changes in the ATRP equilibrium due to lower Br-Cu^{II}/L concentrations with the presence of dormant chains containing EA terminal units. Additional challenges could arise from the fast cross propagation, especially the addition of MMA to the acrylic radical, which can increase dispersity due to higher effective k_p.[71–73]

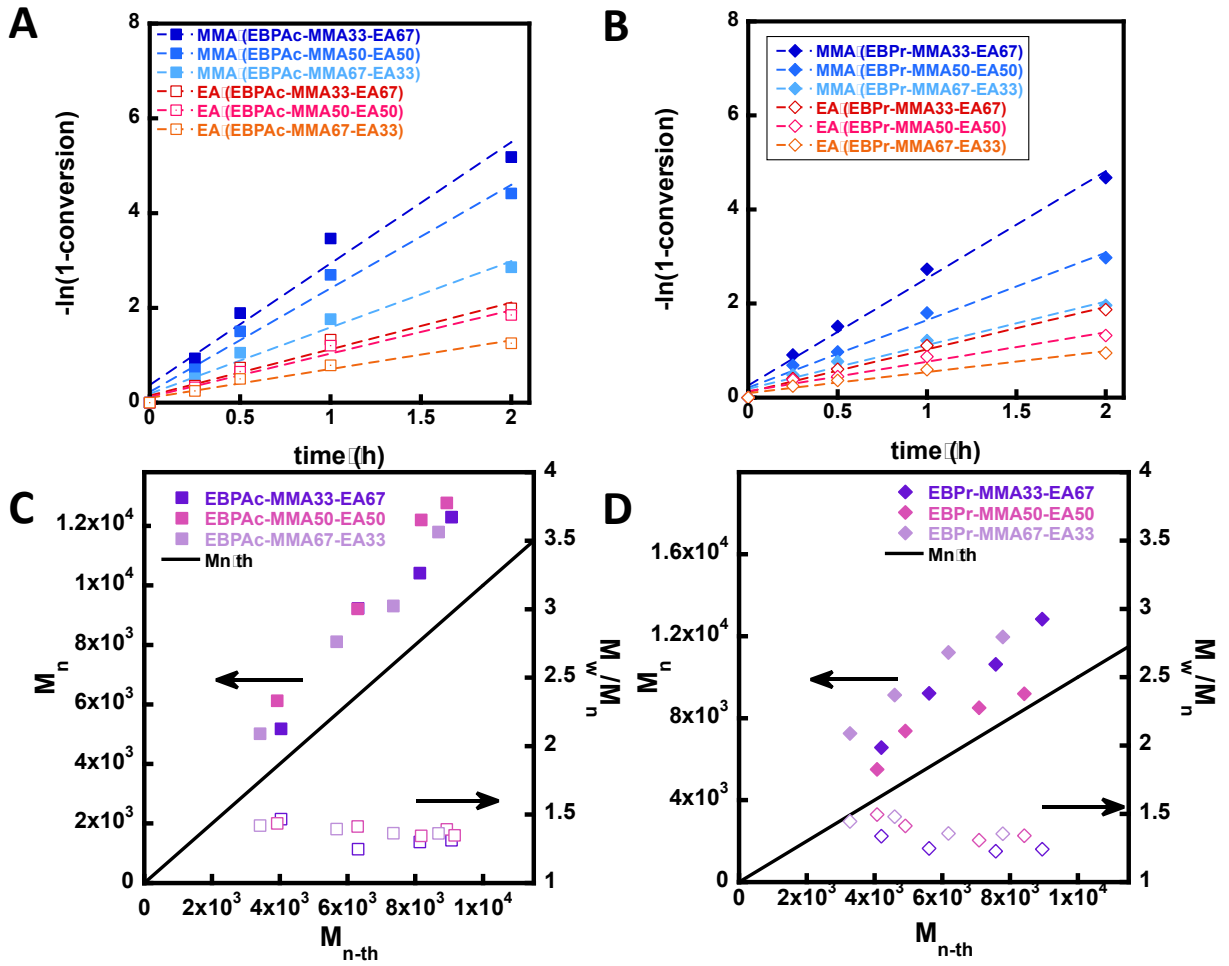

Figure 2: ARGET ATRP MMA-EA gradient polymers at ratios of MMA:EA. Conditions [MMA]:[EA]:[RBr]:[$CuBr_2$]:[Me_6TREN]:[AA]=33:67:1:0.1:0.6:0.2 or [MMA]:[EA]:[RBr]:[$CuBr_2$]:[Me_6TREN]:[AA]=50:50:1:0.1:0.6:0.2 or [MMA]:[EA]:[RBr]:[$CuBr_2$]:[Me_6TREN]:[AA]=67:33:1:0.1:0.6:0.2 in 50 vol % DMSO at 70 °C A) Kinetics of polymerization using RBr=EBPAc. B Kinetics of polymerization using RBr=EBPr. C) Evolution of M_n and M_w/M_n with the $M_{n\text{-}th}$ evaluated from total monomer conversion using

RBr=EBPAc. D) Evolution of M_n and M_w/M_n with the $M_{n\text{-}th}$ evaluated from total monomer conversion using RBr=EBPr.

Figure 3 explores the influence of the total targeted chain length on the polymerization kinetics and the evolution of M_n and dispersity for RAFT systems. Similar to the ATRP systems, the polymerization kinetics were only weakly affected by the CTA structure, both at lower targeted chain length of MMA25-EA25 in Figure 3A and higher targeted chain length of MMA50-EA50 in Figure 3B. These results can be rationalized by the fact that once the RAFT main equilibrium is established, the same propagating radicals and macroCTA are generated from both CPETC and PAETC. The polymerization rate at the lower targeted chain length in Figure 3A is very similar to the rate with the higher targeted chain length in Figure 3B, despite the lower targeted chain length having a higher absolute AIBN concentration. This similarity in rates can be attributed to retardation effects,[74] where the higher CTA concentration increases the rate of radical loss, offsetting the higher AIBN concentration.

The molecular weight evolution data in Figure 3C highlights key discrepancies between the CTAs. The more active CPETC, shows linear evolution and excellent agreement of M_n with $M_{n\text{-}th}$, and relatively low dispersities in the order of 1.2-1.3. In contrast, the less active PAETC CTA has substantial disagreement of M_n vs $M_{n\text{-}th}$, especially at lower conversion and dispersity values in the order of 1.5-1.7. Despite the similarity in monomer consumption rates, the chain initiation is substantially slower for PAETC, leading to poor control over chain length and higher dispersity with the less active leaving group.

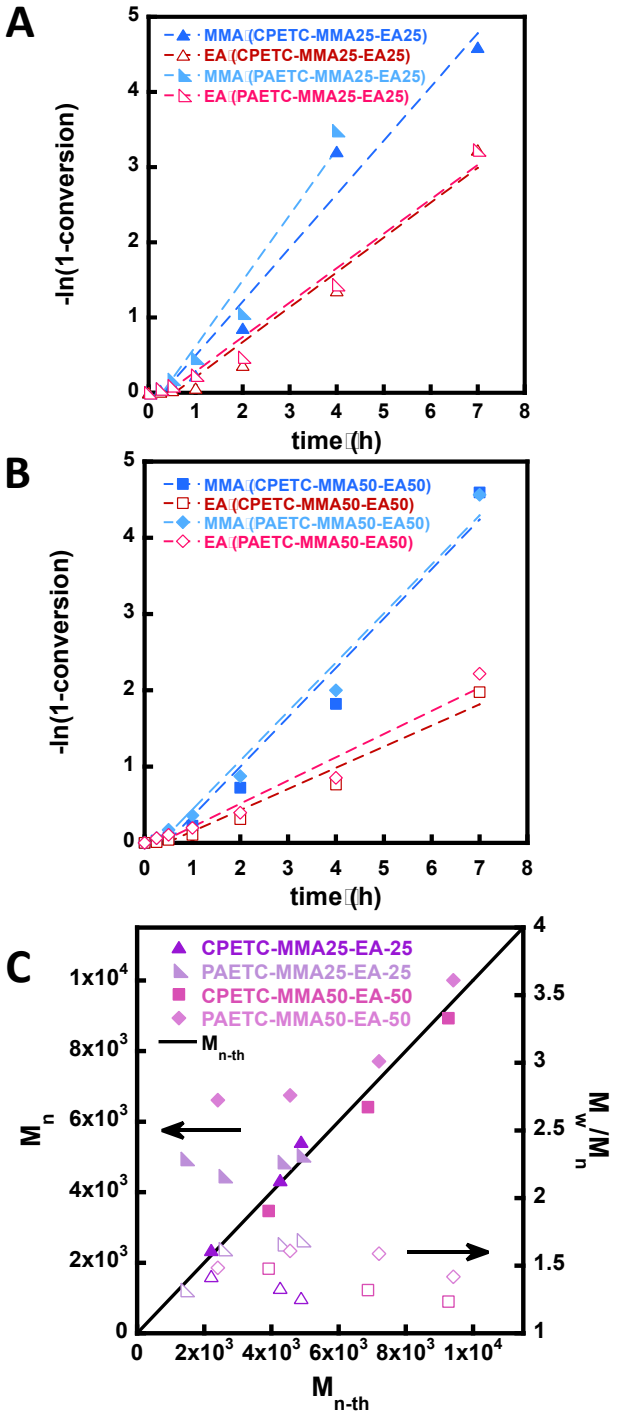

Figure 3: RAFT MMA-EA gradient polymers at different chain lengths. Conditions [MMA]:[EA]:[CTA]:[AIBN]=50:50:1:0.2 or [MMA]:[EA]:[CTA]:[AIBN]=50:50:1:0.2 in 50 vol % DMSO at 70 °C. CTA= CPETC or PAETC. A) Kinetics of polymerization at target chain length of 25 units of MMA and EA. B) Kinetics of polymerization at target chain length of 50 units of MMA and EA. C) Evolution of M_n and M_w/M_n with the $M_{n\text{-}th}$ evaluated from total monomer conversion.

RAFT copolymerization with three different ratios of MMA to EA were explored in Figure 4. Systems with an excess of MMA; MMA67-EA33, equal ratios of MMA and EA; MMA50-EA50, and with an excess of EA; MMA33-EA67 were used. Figure 4A shows that when the more active CPETC CTA is used, which is well suited to the initiation of both MMA and EA chain, the polymerization rate follows the monomer's intrinsic k_p, which has been found to be accurate in related copolymerization systems when using a terminal reactivity model.[75,76] Specifically, systems with higher amounts of the faster propagating EA monomer show substantially higher polymerization rates than those with higher amounts of MMA monomer. The trend for the more active CPETC RAFT CTA follows the trends observed for the ATRP systems which was shown in Figure 2. A more complex trend is observed in Figure 4B for the copolymerization of MMA and EA using the less active PAETC CTA. Although the fastest system is the one with a ratio of MMA:EA = 33:67, the rate of reaction with 67% EA is somewhat higher than the comparable CPETC polymerization, especially at later timepoints in the reaction. When comparing the systems with the higher MMA loading of MMA:EA=50:50 and MMA:EA=67:33, the polymerization rate shows negligible decrease with the higher MMA content. Due to the poor initiation caused by the the poorer propionic acid leaving group for MMA, it is possible that there is a substantial amount of unreacted CTA remaining in the reaction mixture even after substantial monomer conversion has occurred. The lower effective CTA concentration could decrease retardation effects,[74] causing small to negligible decreases in polymerization rate as the MMA concentration increases.

Figure 4C and 4D investigate the evolution of M_n and dispersity with $M_{n\text{-}th}$ for the more active CPETC and less active PAETC systems. When the more active CPETC CTA is used in all ratios of MMA to EA, the M_n evolution is linear and in excellent agreement with $M_{n\text{-}th}$, and dispersity values are in the order of 1.15-1.3. In contrast, when the less active PAETC CTA is used,

the control over M_n is poor, and higher dispersities are observed, particularly at higher ratios of MMA. This suggests that poor chain initiation occurs in the RAFT polymerization with the less active PAETC CTA, and this is especially problematic when higher loadings of the more active MMA monomer are used. This is likely due to slow reaction with MMA-terminal radicals, so that unreacted PAETC remains far into the polymerization reaction with respect to time. In contrast CPETC, which has a better homolytic leaving group, fully converts to macroCTA before substantial polymerization occurs. Slow conversion of PAETC to macroRAFT agent may also explain the higher polymerization rate at higher fractions of MMA, as the presence of a larger fraction of MMA-terminal radicals would result in less efficient conversion of PAETC to macroCTA, thereby reducing the effective CTA concentration and decreasing retardation effects.[62,74] Interestingly, in the RAFT systems with 67% loading of EA, both PAETC and CPETC give well controlled polymers with narrow dispersity and M_n close to $M_{n\text{-th}}$, which is consistent with PAETC being an effective CTA for the homopolymerization of acrylates and acrylamides.[51,52]

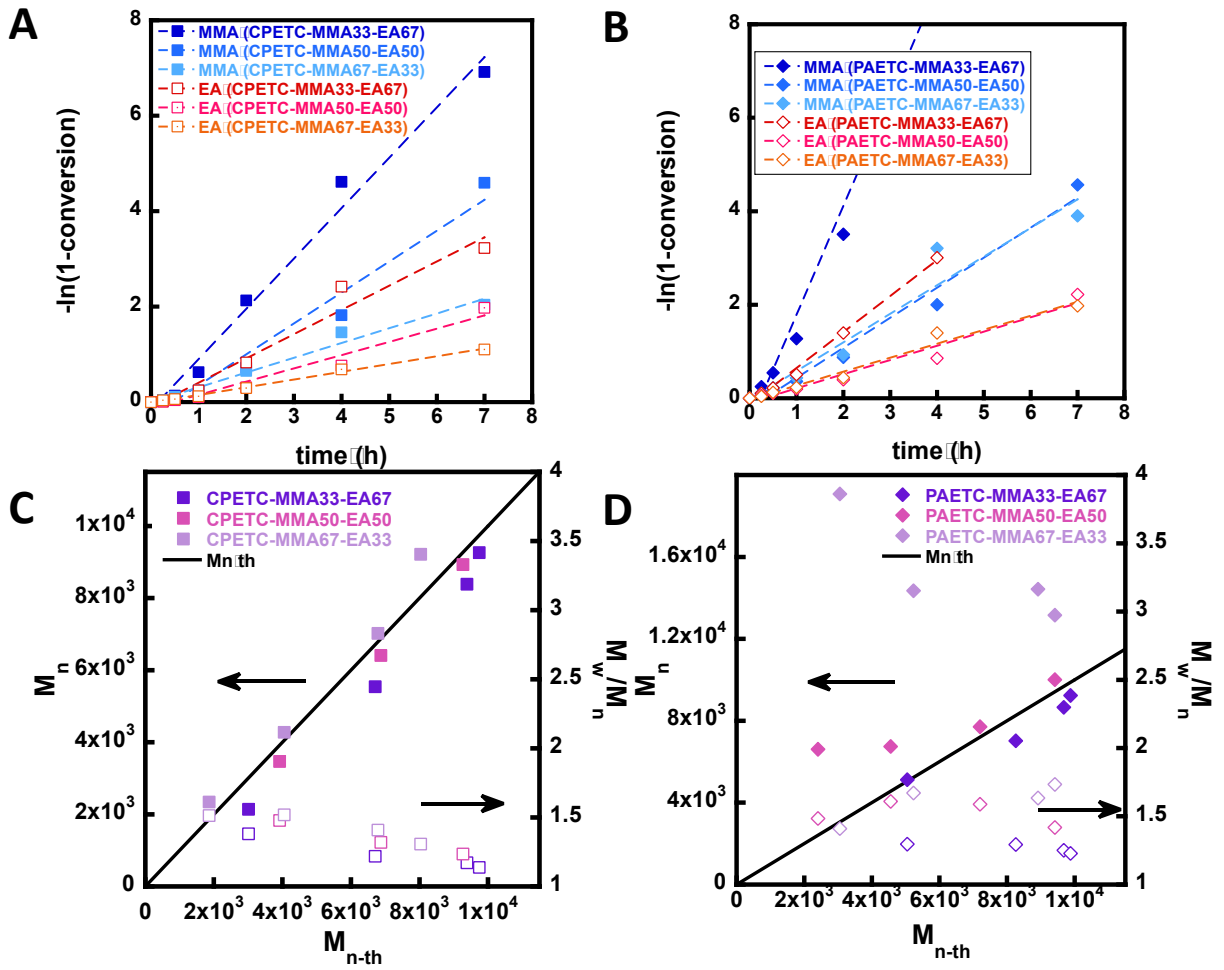

Figure 4: RAFT MMA-EA gradient polymers at ratios of MMA:EA. Conditions [MMA]:[EA]:[CTA]:[AIBN]=33:67:1:0.2 or [MMA]:[EA]:[CTA]:[AIBN]=50:50:1:0.2 or [MMA]:[EA]:[CTA]:[AIBN]=67:33:1:0.2 in 50 vol % DMSO at 70 °C A) Kinetics of polymerization using CTA=CPETC. B Kinetics of polymerization using CTA=PAETC. C) Evolution of M_n and M_w/M_n with the $M_{n\text{-}th}$ evaluated from total monomer conversion using CTA=CPETC. D) Evolution of M_n and M_w/M_n with the $M_{n\text{-}th}$ evaluated from total monomer conversion using CTA=PAETC.

Using the kinetic data in Figures 1-4, and an analogous conventional free radical polymerization system shown in Figure S1, reactivity ratios for each polymerization system and initiator/CTA were determined by fitting the kinetic data to the integrated form of the terminal model copolymer composition equation (the Meyer-Lowry equation[77]). Non-linear least-squares regression[19,78] was used along with visualization of the sum of squares space (details in SI). The fitted reactivity ratios are given in Table 1, and for each system/initiator, as well as the experimental

data and model curves, are given in Figures S2-6. Mole fractions of MMA as a function of conversion for each polymerization method, initiator type and initial composition are given in Figures S7-11. In all cases, the reactivity ratios are consistent with the kinetic data, showing strong gradient characteristics as r_{MMA} is between 1.4-1.9 and r_{EA} is between 0.25-0.35.[67] However, each system in Table 1 has distinct reactivity characteristics. The two RAFT (CPETC and PAETC) systems and the ATRP using EBPr give r_{MMA}~1.65-1.85 and r_{EA}~0.3-0.4.

It is important to note that r_{MMA} in all systems is in the order of 1.7-1.85, with the discrepancy between the ATRP and RAFT initiation systems and the free radical polymerization (FRP) model experiment being relatively small. Similarly, the r_{EA} is similar when comparing the less and more active initiators/CTAs in RAFT and ATRP as well as by a comparable FRP model system.

Using the reactivity ratios in Table 1, idealized polymer composition diagrams for 10 representative polymer chains were also simulated.[19] These simulations do not take into account distributions in chain length but are useful in visualizing how the discrete monomer units may be distributed in a chain, and the typical variation from one chain to another. Full details of the simulation algorithm are given in the SI. The comparison of the four polymerization systems (ATRP with EBPAc or EBPr and RAFT with CPETC or PAETC) at each targeted chain length and monomer loading is given in Figure S12. Despite the variations in reactivity ratios, the simulated polymer chains were similar for all systems. Figure 5 shows simulated polymer chains for the best controlled system, RAFT using CPETC as the initiator, for each monomer feed and chain length studied. As seen in Figure 5, the strongest gradient like characteristics were found in systems with initial loading of MMA equal to 33% or 50%. While the system having 67% of MMA in the initial feed having lower conversion and consequently less gradient character.

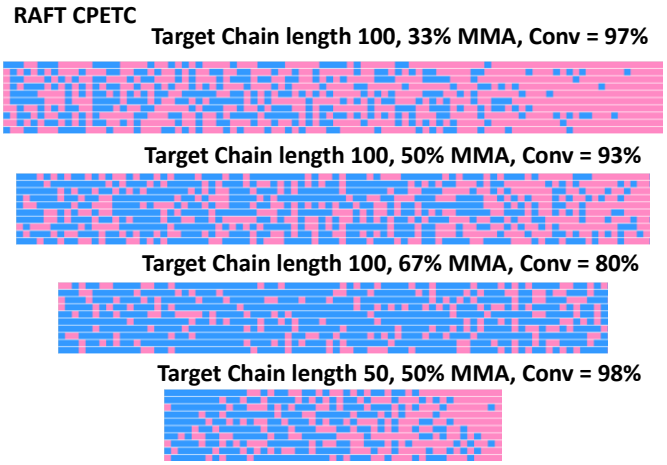

Figure 5: Simulated composition of 10 chains using r_{MMA} = 1.86 and r_{EA} = 0.30, consistent with the RAFT polymerization of using CPETC as the CTA. Composition and chain length are varied.

Table 1: Reactivity ratios of MMA – EA system at 70 °C with distinct initiation and control methods. [64]

System	Initiator/CTA	r_{MMA}	r_{EA}
ATRP	EBPAc	1.82	0.35
ATRP	EBPr	1.78	0.35
RAFT	CPETC	1.86	0.30
RAFT	PAETC	1.69	0.29
FRP	DDM	1.77	0.38

In analyzing the data in Figures 1-4 and Table 1, several preliminary conclusions can be drawn. Unlike homopolymerization of acrylates and methacrylates by ATRP, which can reliably be performed in a controlled manner with 100 ppm or less of Cu catalyst, the copolymerization of acrylates and methacrylates requires substantially higher catalyst loadings for control, in the order of 1000 ppm, which is qualitatively similar to previous reports on spontaneous gradient copolymers by ARGET ATRP.[47] This is likely due to distortions of the ATRP equilibrium and possible enhancements of propagation, especially from acrylic radicals adding MMA, and reduced deactivation efficiency of these methacrylic radicals. Even at these high catalyst loadings, control over chain length and dispersity are relatively poor, with measurable and consistent deviations of M_n compared to $M_{n\text{-}th}$, and dispersities between 1.3 and 1.5 for most ATRP gradient systems.

However, the influence of initiator (EBPAc vs EBPr) is relatively minor, due to high rates of ATRP activation from the high catalyst loading. Presumably even higher catalyst loadings would be required to reduce the dispersity, although at that point the catalyst loading would be near stoichiometric with the chain end, which goes against the principles of ARGET ATRP ppm catalyst loadings.[57–59] The relatively poor correlation of M_n with $M_{n\text{-}th}$ is consistent with some slower initiation, or loss of the ATRP to irreversible termination reactions at very low conversion. The linear increase of M_n with conversion, is more consistent with the latter phenomenon, where some initiating chains terminate early in the reaction before the main ATRP equilibrium is established.

In the case of RAFT gradient polymers, the design principles are substantially simpler. The more active CPETC CTA leads to good control over the polymerization, with excellent correlation of M_n with $M_{n\text{-}th}$, and dispersities in the order of 1.15-1.3. CPETC CTA can be used for the homopolymerization of both acrylic and methacrylic monomers, due to effective establishment of the RAFT main equilibrium at relatively low total conversion. In contrast, the less active PAETC leads to systematic deviations of M_n from $M_{n\text{-}th}$, slow initiation, and higher dispersities. This is especially apparent at higher ratios of MMA, for which PAETC is expected to be an incompatible CTA.[61,79] Only the 67% EA system gave efficient control of the polymerization.[80] This is surprising because even an initial feed containing 67% of MMA also contains 33% of EA. Furthermore, EA is incorporated into the copolymer from the early stages of polymerization, as seen in the simulations of Figure S12. In principle the acrylic acid leaving group of PAETC should have similar reactivity to an acrylate terminated chain. The slow conversion of PAETC to macroCTA in the copolymerization of MMA/EA is likely due to a combination of the following effects: i) the methacrylic radical should be the dominant radical species in these copolymerizations especially at low conversion; ii) penultimate unit effects increasing the reactivity of the acrylic terminated

polymer; and iii) steric effects which could make the small molecule PAETC less efficient as a CTA than the acrylate terminated chain. From the calculated reactivity ratios in Table 1, the dominant radical species is the methacrylic radical. Even though acrylate monomers add to the methacrylic radical at relatively low conversion (Figure S12), the rapidly propagating acrylic chain ends [81] are more likely to add methacrylic monomers. Addition of MMA to the acrylic radical—forming a methacrylic radical which is unreactive towards PAETC—is competitive with the reaction of the acrylic radical with the PAETC CTA, reducing the efficiency of conversion of PAETC to macroCTA. Steric effects could make the smaller propionic acid leaving group less efficient than the acrylate terminated polymer chain, further reducing initiation efficiency. Finally, in an acrylate terminated polymer the penultimate unit is almost always a methacrylic unit at low conversion in MMA/EA copolymerization. This methacrylic penultimate unit could increase the reactivity of the acrylic terminated chain, similar to how methacrylic polymer are more active ATRP initiators than their monomers.[82–84] This could make the polymer more likely to fragment in the RAFT intermediate compared to the acrylic acid leaving group, however, a full penultimate unit analysis is beyond the scope of this work.[80]

One of the most interesting findings of the spontaneous gradient study of MMA and EA by both RAFT and ATRP is that careful design of the reaction conditions is needed. In particular, simple extrapolation of conditions that work for either MMA or EA may not always apply to the complex copolymerization due to the presence of the two distinct radical chain ends; the more reactive acrylic radical compared to the less reactive methacrylic radical. The ATRP and RAFT processes also generate two distinct dormant chains, a more difficult to activate acrylic chain end and an easier to activate methacrylic chain end. For both the efficient deactivation of the

methacrylic radicals and the activation of the acrylic chain ends, an order of magnitude higher Cu catalyst loading was needed in gradient ATRP, compared to homopolymerization (Table S2). [57,59]

In the case of RAFT, only CPETC, the CTA that gives efficient control over both homopolymerizations, gave well controlled gradient polymers, due to poor initiation and fragmentation of the less reactive acrylic acid leaving group in PAETC. Even 50% loading of the acrylate monomer, EA, the reaction still led to slow initiation and high dispersity polymers. This is quite distinct from nitroxide-mediated polymerization (NMP), where even a small fraction ~10% of the compatible monomer styrene led to well controlled polymerization of MMA.[85,86] The difference most likely is due to the substantially different reactivity ratios in MMA/EA and the rapid propagation rate of EA compared to MMA, which suggest that the ratio of EA-terminal radicals to MMA-terminal radicals will be low, especially at low conversion.

Conclusions

A series of spontaneous gradient polymers of MMA and EA as model systems to compare methacrylic and acrylic monomers were prepared by both ARGET ATRP and thermally initiated RAFT polymerization. Comparison of RAFT and ATRP across a range of conditions indicates that the simplest design of gradient polymers based on methacrylic/acrylic monomers appears to be the RAFT system that uses a CTA compatible with both monomers, such as CPETC. The poorest choice is RAFT polymerization with a CTA that is incompatible with the more reactive monomer due to the slow formation of the macroCTA, leading to dispersities over 1.5. ATRP with high catalyst loading (~1000 ppm) gives relatively well controlled polymers, with linear increase of M_n with conversion, although somewhat above $M_{n\text{-}th}$, and higher dispersities than the well-controlled RAFT system that uses CPETC. The RAFT polymerization of MMA and EA using CPETC leads to efficient initiation, superior correlation of M_n with $M_{n\text{-}th}$, and the consistently lowest dispersity

values. Simulations based on calculated reactivity ratios indicate that the chains typically have gradient like properties, especially at equal or higher loadings of the acrylic monomer.

Conflicts of Interest

The authors declare no competing interests

Acknowledgements

This work was partially supported by the National Science Foundation under award number CHE-2203727. RDG was supported through the National Science Foundation Research Experiences for Undergraduates (REU) program under award number CHE-1851795.

Author Contributions

K.G.E.B., R.D.G. and M.A.S.N.W. were involved in experimental design, data acquisition, formal analysis and writing and editing. S.H. was involved in experimental design, formal analysis and writing and editing. D.K. was involved in conceptualization, experimental design, formal analysis and writing and editing.

References

(1) Qiu, L. Y.; Bae, Y. H. Polymer Architecture and Drug Delivery. *Pharm Res* **2006**, *23* (1), 1–30. https://doi.org/10.1007/s11095-005-9046-2.

(2) McLeish, T. C. B. Polymer Architecture Influence on Rheology. *Curr Opin Solid State Mater Sci* **1997**, *2* (6), 678–682. https://doi.org/https://doi.org/10.1016/S1359-0286(97)80009-5.

(3) Stals, P. J. M.; Li, Y.; Burdyńska, J.; Nicolaÿ, R.; Nese, A.; Palmans, A. R. A.; Meijer, E. W.; Matyjaszewski, K.; Sheiko, S. S. How Far Can We Push Polymer Architectures? *J Am Chem Soc* **2013**, *135* (31), 11421–11424. https://doi.org/10.1021/ja400890v.

(4) De Alwis Watuthanthrige, N.; Chakma, P.; Konkolewicz, D. Designing Dynamic Materials from Dynamic Bonds to Macromolecular Architecture. *Trends Chem* **2021**, *3* (3), 231–247. https://doi.org/10.1016/j.trechm.2020.12.005.

(5) Matyjaszewski, K. Architecturally Complex Polymers with Controlled Heterogeneity. *Science (1979)* **2011**, *333* (6046), 1104–1105. https://doi.org/10.1126/science.1209660.

(6) Gregory, A.; Stenzel, M. H. Complex Polymer Architectures via RAFT Polymerization: From Fundamental Process to Extending the Scope Using Click Chemistry and Nature's Building Blocks. *Prog Polym Sci* **2012**, *37* (1), 38–105. https://doi.org/https://doi.org/10.1016/j.progpolymsci.2011.08.004.

(7) Davis, K. A.; Matyjaszewski, K. Statistical, Gradient, Block, and Graft Copolymers by Controlled/Living Radical Polymerizations. In *Statistical, Gradient, Block and Graft Copolymers by Controlled/Living Radical Polymerizations*; Matyjaszewski, K., Davis, K. A., Eds.; Springer Berlin Heidelberg: Berlin, Heidelberg, 2002; pp 1–13. https://doi.org/10.1007/3-540-45806-9_1.
(8) Matyjaszewski, K. Advanced Materials by Atom Transfer Radical Polymerization. *Advanced Materials* **2018**, *30* (23), 1706441. https://doi.org/https://doi.org/10.1002/adma.201706441.
(9) Matyjaszewski, K.; Ziegler, M. J.; Arehart, S. V; Greszta, D.; Pakula, T. Gradient Copolymers by Atom Transfer Radical Copolymerization. *J Phys Org Chem* **2000**, *13* (12), 775–786. https://doi.org/https://doi.org/10.1002/1099-1395(200012)13:12<775::AID-POC314>3.0.CO;2-D.
(10) Kryszewski, M. Gradient Polymers and Copolymers. *Polym Adv Technol* **1998**, *9* (4), 244–259. https://doi.org/https://doi.org/10.1002/(SICI)1099-1581(199804)9:4<244::AID-PAT748>3.0.CO;2-J.
(11) Claussen, K. U.; Scheibel, T.; Schmidt, H.-W.; Giesa, R. Polymer Gradient Materials: Can Nature Teach Us New Tricks? *Macromol Mater Eng* **2012**, *297* (10), 938–957. https://doi.org/https://doi.org/10.1002/mame.201200032.
(12) Zhang, Y.; Tang, Y.; Zhang, J.; Harrisson, S. Amphiphilic Asymmetric Diblock Copolymer with PH-Responsive Fluorescent Properties. *ACS Macro Lett* **2021**, *10* (11), 1346–1352. https://doi.org/10.1021/acsmacrolett.1c00553.
(13) Liu, X.; Wang, M.; Harrisson, S.; Debuigne, A.; Marty, J.-D.; Destarac, M. Enhanced Stabilization of Water/ScCO2 Interface by Block-Like Spontaneous Gradient Copolymers. *ACS Sustain Chem Eng* **2017**, *5* (11), 9645–9650. https://doi.org/10.1021/acssuschemeng.7b02779.
(14) Ercole, F.; Malic, N.; Harrisson, S.; Davis, T. P.; Evans, R. A. Photochromic Polymer Conjugates: The Importance of Macromolecular Architecture in Controlling Switching Speed within a Polymer Matrix. *Macromolecules* **2010**, *43* (1), 249–261. https://doi.org/10.1021/ma901830b.
(15) Yañez-Macias, R.; Kulai, I.; Ulbrich, J.; Yildirim, T.; Sungur, P.; Hoeppener, S.; Guerrero-Santos, R.; Schubert, U. S.; Destarac, M.; Guerrero-Sanchez, C.; Harrisson, S. Thermosensitive Spontaneous Gradient Copolymers with Block- and Gradient-like Features. *Polym Chem* **2017**, *8* (34), 5023–5032. https://doi.org/10.1039/C7PY00495H.
(16) Beckingham, B. S.; Sanoja, G. E.; Lynd, N. A. Simple and Accurate Determination of Reactivity Ratios Using a Nonterminal Model of Chain Copolymerization. *Macromolecules* **2015**, *48* (19), 6922–6930. https://doi.org/10.1021/acs.macromol.5b01631.
(17) Kim, J.; Mok, M. M.; Sandoval, R. W.; Woo, D. J.; Torkelson, J. M. Uniquely Broad Glass Transition Temperatures of Gradient Copolymers Relative to Random and Block Copolymers Containing Repulsive Comonomers. *Macromolecules* **2006**, *39* (18), 6152–6160. https://doi.org/10.1021/ma061241f.
(18) Zhang, J.; Farias-Mancilla, B.; Kulai, I.; Hoeppener, S.; Lonetti, B.; Prévost, S.; Ulbrich, J.; Destarac, M.; Colombani, O.; Schubert, U. S.; Guerrero-Sanchez, C.; Harrisson, S. Effect of Hydrophilic Monomer Distribution on Self-Assembly of a PH-Responsive Copolymer: Spheres, Worms and Vesicles from a Single Copolymer Composition.

Angewandte Chemie International Edition **2021**, *60* (9), 4925–4930. https://doi.org/https://doi.org/10.1002/anie.202010501.
(19) Harrisson, S.; Ercole, F.; Muir, B. W. Living Spontaneous Gradient Copolymers of Acrylic Acid and Styrene: One-Pot Synthesis of PH-Responsive Amphiphiles. *Polym Chem* **2010**, *1* (3), 326–332. https://doi.org/10.1039/B9PY00301K.
(20) Farias-Mancilla, B.; Zhang, J.; Kulai, I.; Destarac, M.; Schubert, U. S.; Guerrero-Sanchez, C.; Harrisson, S.; Colombani, O. Gradient and Asymmetric Copolymers: The Role of the Copolymer Composition Profile in the Ionization of Weak Polyelectrolytes. *Polym Chem* **2020**, *11* (47), 7562–7570. https://doi.org/10.1039/D0PY01059F.
(21) Okabe, S.; Seno, K.; Kanaoka, S.; Aoshima, S.; Shibayama, M. Micellization Study on Block and Gradient Copolymer Aqueous Solutions by DLS and SANS. *Macromolecules* **2006**, *39* (4), 1592–1597. https://doi.org/10.1021/ma052334k.
(22) Kravchenko, V. S.; Potemkin, I. I. Micelles of Gradient vs Diblock Copolymers: Difference in the Internal Structure and Properties. *J Phys Chem B* **2016**, *120* (47), 12211–12217. https://doi.org/10.1021/acs.jpcb.6b10120.
(23) Mok, M. M.; Kim, J.; Torkelson, J. M. Gradient Copolymers with Broad Glass Transition Temperature Regions: Design of Purely Interphase Compositions for Damping Applications. *J Polym Sci B Polym Phys* **2008**, *46* (1), 48–58. https://doi.org/https://doi.org/10.1002/polb.21341.
(24) Kim, J.; Gray, M. K.; Zhou, H.; Nguyen, S. T.; Torkelson, J. M. Polymer Blend Compatibilization by Gradient Copolymer Addition during Melt Processing: Stabilization of Dispersed Phase to Static Coarsening. *Macromolecules* **2005**, *38* (4), 1037–1040. https://doi.org/10.1021/ma047549t.
(25) Zheng, C. Gradient Copolymer Micelles: An Introduction to Structures as Well as Structural Transitions. *Soft Matter* **2019**, *15* (27), 5357–5370. https://doi.org/10.1039/C9SM00880B.
(26) Okabe, S.; Seno, K.; Kanaoka, S.; Aoshima, S.; Shibayama, M. Micellization Study on Block and Gradient Copolymer Aqueous Solutions by DLS and SANS. *Macromolecules* **2006**, *39* (4), 1592–1597. https://doi.org/10.1021/ma052334k.
(27) Shanmugam, S.; Boyer, C. Stereo-, Temporal and Chemical Control through Photoactivation of Living Radical Polymerization: Synthesis of Block and Gradient Copolymers. *J Am Chem Soc* **2015**, *137* (31), 9988–9999. https://doi.org/10.1021/jacs.5b05903.
(28) Corrigan, N.; Jung, K.; Moad, G.; Hawker, C. J.; Matyjaszewski, K.; Boyer, C. Reversible-Deactivation Radical Polymerization (Controlled/Living Radical Polymerization): From Discovery to Materials Design and Applications. *Prog Polym Sci* **2020**, *111*, 101311. https://doi.org/https://doi.org/10.1016/j.progpolymsci.2020.101311.
(29) Parkatzidis, K.; Wang, H. S.; Truong, N. P.; Anastasaki, A. Recent Developments and Future Challenges in Controlled Radical Polymerization: A 2020 Update. *Chem* **2020**, *6* (7), 1575–1588. https://doi.org/https://doi.org/10.1016/j.chempr.2020.06.014.
(30) Truong, N. P.; Jones, G. R.; Bradford, K. G. E.; Konkolewicz, D.; Anastasaki, A. A Comparison of RAFT and ATRP Methods for Controlled Radical Polymerization. *Nat Rev Chem* **2021**, *5* (12), 859–869. https://doi.org/10.1038/s41570-021-00328-8.
(31) Lefay, C.; Charleux, B.; Save, M.; Chassenieux, C.; Guerret, O.; Magnet, S. Amphiphilic Gradient Poly(Styrene-Co-Acrylic Acid) Copolymer Prepared via Nitroxide-Mediated Solution Polymerization. Synthesis, Characterization in Aqueous Solution and Evaluation

as Emulsion Polymerization Stabilizer. *Polymer (Guildf)* **2006**, *47* (6), 1935–1945. https://doi.org/https://doi.org/10.1016/j.polymer.2006.01.034.
(32) Zhang, J.; Farias-Mancilla, B.; Destarac, M.; Schubert, U. S.; Keddie, D. J.; Guerrero-Sanchez, C.; Harrisson, S. Asymmetric Copolymers: Synthesis, Properties, and Applications of Gradient and Other Partially Segregated Copolymers. *Macromol Rapid Commun* **2018**, *39* (19), 1800357. https://doi.org/https://doi.org/10.1002/marc.201800357.
(33) Guerrero-Sanchez, C.; Harrisson, S.; Keddie, D. J. High-Throughput Method for RAFT Kinetic Investigations and Estimation of Reactivity Ratios in Copolymerization Systems. *Macromol Symp* **2013**, *325–326* (1), 38–46. https://doi.org/https://doi.org/10.1002/masy.201200038.
(34) Harrisson, S.; Wooley, K. L. Shell-Crosslinked Nanostructures from Amphiphilic AB and ABA Block Copolymers of Styrene-Alt-(Maleic Anhydride) and Styrene: Polymerization, Assembly and Stabilization in One Pot. *Chemical Communications* **2005**, No. 26, 3259–3261. https://doi.org/10.1039/B504313A.
(35) Sykes, K. J.; Harrisson, S.; Keddie, D. J. Phosphorus-Containing Gradient (Block) Copolymers via RAFT Polymerization and Postpolymerization Modification. *Macromol Chem Phys* **2016**, *217* (20), 2310–2320. https://doi.org/https://doi.org/10.1002/macp.201600087.
(36) Burridge, K. M.; De Alwis Watuthanthrige, N.; Payne, C.; Page, R. C.; Konkolewicz, D. Simple Polymerization through Oxygen at Reduced Volumes Using Oil and Water. *Journal of Polymer Science* **2021**, *59* (21), 2530–2536. https://doi.org/https://doi.org/10.1002/pol.20210386.
(37) Alshehri, I. H.; Pahovnik, D.; Žagar, E.; Shipp, D. A. Stepwise Gradient Copolymers of N-Butyl Acrylate and Isobornyl Acrylate by Emulsion RAFT Copolymerizations. *Macromolecules* **2022**, *55* (2), 391–400. https://doi.org/10.1021/acs.macromol.1c01897.
(38) Sun, X.; Luo, Y.; Wang, R.; Li, B.-G.; Liu, B.; Zhu, S. Programmed Synthesis of Copolymer with Controlled Chain Composition Distribution via Semibatch RAFT Copolymerization. *Macromolecules* **2007**, *40* (4), 849–859. https://doi.org/10.1021/ma061677v.
(39) Steinhauer, W.; Hoogenboom, R.; Keul, H.; Moeller, M. Block and Gradient Copolymers of 2-Hydroxyethyl Acrylate and 2-Methoxyethyl Acrylate via RAFT: Polymerization Kinetics, Thermoresponsive Properties, and Micellization. *Macromolecules* **2013**, *46* (4), 1447–1460. https://doi.org/10.1021/ma302606x.
(40) Escalé, P.; Ting, S. R. S.; Khoukh, A.; Rubatat, L.; Save, M.; Stenzel, M. H.; Billon, L. Synthetic Route Effect on Macromolecular Architecture: From Block to Gradient Copolymers Based on Acryloyl Galactose Monomer Using RAFT Polymerization. *Macromolecules* **2011**, *44* (15), 5911–5919. https://doi.org/10.1021/ma201208u.
(41) D'hooge, D. R.; Van Steenberge, P. H. M.; Reyniers, M.-F.; Marin, G. B. Fed-Batch Control and Visualization of Monomer Sequences of Individual ICAR ATRP Gradient Copolymer Chains. *Polymers (Basel)* **2014**, *6* (4), 1074–1095.
(42) Min, K.; Li, M.; Matyjaszewski, K. Preparation of Gradient Copolymers via ATRP Using a Simultaneous Reverse and Normal Initiation Process. I. Spontaneous Gradient. *J Polym Sci A Polym Chem* **2005**, *43* (16), 3616–3622. https://doi.org/https://doi.org/10.1002/pola.20809.
(43) Van Steenberge, P. H. M.; D'hooge, D. R.; Wang, Y.; Zhong, M.; Reyniers, M.-F.; Konkolewicz, D.; Matyjaszewski, K.; Marin, G. B. Linear Gradient Quality of ATRP

Copolymers. *Macromolecules* **2012**, *45* (21), 8519–8531. https://doi.org/10.1021/ma3017597.
(44) Wang, R.; Luo, Y.; Li, B.-G.; Zhu, S. Control of Gradient Copolymer Composition in ATRP Using Semibatch Feeding Policy. *AIChE Journal* **2007**, *53* (1), 174–186. https://doi.org/https://doi.org/10.1002/aic.11063.
(45) Beginn, U. Gradient Copolymers. *Colloid Polym Sci* **2008**, *286* (13), 1465–1474. https://doi.org/10.1007/s00396-008-1922-y.
(46) Cuthbert, J.; Wanasinghe, S. V; Matyjaszewski, K.; Konkolewicz, D. Are RAFT and ATRP Universally Interchangeable Polymerization Methods in Network Formation? *Macromolecules* **2021**, *54* (18), 8331–8340. https://doi.org/10.1021/acs.macromol.1c01587.
(47) Elsen, A. M.; Li, Y.; Li, Q.; Sheiko, S. S.; Matyjaszewski, K. Exploring Quality in Gradient Copolymers. *Macromol Rapid Commun* **2014**, *35* (2), 133–140. https://doi.org/https://doi.org/10.1002/marc.201300654.
(48) Lee, H.; Matyjaszewski, K.; Yu, S.; Sheiko, S. S. Molecular Brushes with Spontaneous Gradient by Atom Transfer Radical Polymerization. *Macromolecules* **2005**, *38* (20), 8264–8271. https://doi.org/10.1021/ma051231z.
(49) Vakil, J. R.; De Alwis Watuthanthrige, N.; Digby, Z. A.; Zhang, B.; Lacy, H. A.; Sparks, J. L.; Konkolewicz, D. Controlling Polymer Architecture to Design Dynamic Network Materials with Multiple Dynamic Linkers. *Mol Syst Des Eng* **2020**, *5* (7), 1267–1276. https://doi.org/10.1039/D0ME00015A.
(50) Zhang, B.; Ke, J.; Vakil, J. R.; Cummings, S. C.; Digby, Z. A.; Sparks, J. L.; Ye, Z.; Zanjani, M. B.; Konkolewicz, D. Dual-Dynamic Interpenetrated Networks Tuned through Macromolecular Architecture. *Polym Chem* **2019**, *10* (46), 6290–6304. https://doi.org/10.1039/C9PY01387C.
(51) Wright, T. A.; Bennett, C.; Johnson, M. R.; Fischesser, H.; Chandrarathne, B. M.; Ram, N.; Maloof, E.; Tyler, A.; Upshaw, C. R.; Stewart, J. M.; Page, R. C.; Konkolewicz, D. Investigating the Impact of Polymer Length, Attachment Site, and Charge on Enzymatic Activity and Stability of Cellulase. *Biomacromolecules* **2022**, *23* (10), 4097–4109. https://doi.org/10.1021/acs.biomac.2c00441.
(52) Wright, T. A.; Lucius Dougherty, M.; Schmitz, B.; Burridge, K. M.; Makaroff, K.; Stewart, J. M.; Fischesser, H. D.; Shepherd, J. T.; Berberich, J. A.; Konkolewicz, D.; Page, R. C. Polymer Conjugation to Enhance Cellulase Activity and Preserve Thermal and Functional Stability. *Bioconjug Chem* **2017**, *28* (10), 2638–2645. https://doi.org/10.1021/acs.bioconjchem.7b00518.
(53) Lucius, M.; Falatach, R.; McGlone, C.; Makaroff, K.; Danielson, A.; Williams, C.; Nix, J. C.; Konkolewicz, D.; Page, R. C.; Berberich, J. A. Investigating the Impact of Polymer Functional Groups on the Stability and Activity of Lysozyme–Polymer Conjugates. *Biomacromolecules* **2016**, *17* (3), 1123–1134. https://doi.org/10.1021/acs.biomac.5b01743.
(54) Nwoko, T.; De Alwis Watuthanthrige, N.; Parnitzke, B.; Yehl, K.; Konkolewicz, D. Tuning the Molecular Weight Distributions of Vinylketone-Based Polymers Using RAFT Photopolymerization and UV Photodegradation. *Polym Chem* **2021**, *12* (46), 6761–6770. https://doi.org/10.1039/D1PY01129D.

(55) Matyjaszewski, K. Atom Transfer Radical Polymerization (ATRP): Current Status and Future Perspectives. *Macromolecules* **2012**, *45* (10), 4015–4039. https://doi.org/10.1021/ma3001719.
(56) Harrisson, S.; Nicolas, J. In the (Very) Long Run We Are All Dead: Activation and Termination in SET-LRP/SARA-ATRP. *ACS Macro Lett* **2014**, *3* (7), 643–647. https://doi.org/10.1021/mz500305j.
(57) Chan, N.; Cunningham, M. F.; Hutchinson, R. A. ARGET ATRP of Methacrylates and Acrylates with Stoichiometric Ratios of Ligand to Copper. *Macromol Chem Phys* **2008**, *209* (17), 1797–1805. https://doi.org/https://doi.org/10.1002/macp.200800328.
(58) Matyjaszewski, K.; Dong, H.; Jakubowski, W.; Pietrasik, J.; Kusumo, A. Grafting from Surfaces for "Everyone": ARGET ATRP in the Presence of Air. *Langmuir* **2007**, *23* (8), 4528–4531. https://doi.org/10.1021/la063402e.
(59) Kwak, Y.; Magenau, A. J. D.; Matyjaszewski, K. ARGET ATRP of Methyl Acrylate with Inexpensive Ligands and Ppm Concentrations of Catalyst. *Macromolecules* **2011**, *44* (4), 811–819. https://doi.org/10.1021/ma102665c.
(60) Chiefari, J.; Chong, Y. K. (Bill); Ercole, F.; Krstina, J.; Jeffery, J.; Le, T. P. T.; Mayadunne, R. T. A.; Meijs, G. F.; Moad, C. L.; Moad, G.; Rizzardo, E.; Thang, S. H. Living Free-Radical Polymerization by Reversible Addition−Fragmentation Chain Transfer: The RAFT Process. *Macromolecules* **1998**, *31* (16), 5559–5562. https://doi.org/10.1021/ma9804951.
(61) Perrier, S. 50th Anniversary Perspective: RAFT Polymerization—A User Guide. *Macromolecules* **2017**, *50* (19), 7433–7447. https://doi.org/10.1021/acs.macromol.7b00767.
(62) Barner-Kowollik, C.; Buback, M.; Charleux, B.; Coote, M. L.; Drache, M.; Fukuda, T.; Goto, A.; Klumperman, B.; Lowe, A. B.; Mcleary, J. B.; Moad, G.; Monteiro, M. J.; Sanderson, R. D.; Tonge, M. P.; Vana, P. Mechanism and Kinetics of Dithiobenzoate-Mediated RAFT Polymerization. I. The Current Situation. *J Polym Sci A Polym Chem* **2006**, *44* (20), 5809–5831. https://doi.org/https://doi.org/10.1002/pola.21589.
(63) Mayo, F. R.; Walling, C. Copolymerization. *Chem Rev* **1950**, *46* (2), 191–287.
(64) Davis, T. P. The Mechanism of Propagation in Free-Radical Copolymerization. *J Polym Sci A Polym Chem* **2001**, *39* (5), 597–603. https://doi.org/https://doi.org/10.1002/1099-0518(20010301)39:5<597::AID-POLA1030>3.0.CO;2-Q.
(65) Mao, R.; Huglin, M. B. A New Linear Method to Calculate Monomer Reactivity Ratios by Using High Conversion Copolymerization Data: Terminal Model. *Polymer (Guildf)* **1993**, *34* (8), 1709–1715. https://doi.org/https://doi.org/10.1016/0032-3861(93)90331-4.
(66) Berger, M.; Kuntz, I. The Distinction between Terminal and Penultimate Copolymerization Models. *J Polym Sci A* **1964**, *2* (4), 1687–1698. https://doi.org/https://doi.org/10.1002/pol.1964.100020413.
(67) Madruga, E. L.; San Román, J.; Rodriguez, Ma. J. The Effect of Temperature on the Free Radical Copolymerization of Methyl Methacrylate with Ethyl Acrylate. *Eur Polym J* **1982**, *18* (11), 1011–1013. https://doi.org/https://doi.org/10.1016/0014-3057(82)90091-X.
(68) Tang, W.; Kwak, Y.; Braunecker, W.; Tsarevsky, N. V; Coote, M. L.; Matyjaszewski, K. Understanding Atom Transfer Radical Polymerization: Effect of Ligand and Initiator Structures on the Equilibrium Constants. *J Am Chem Soc* **2008**, *130* (32), 10702–10713. https://doi.org/10.1021/ja802290a.

(69) Haven, J. J.; De Neve, J. A.; Junkers, T. Versatile Approach for the Synthesis of Sequence-Defined Monodisperse 18- and 20-Mer Oligoacrylates. *ACS Macro Lett* **2017**, *6* (7), 743–747. https://doi.org/10.1021/acsmacrolett.7b00430.
(70) Falatach, R.; McGlone, C.; Al-Abdul-Wahid, M. S.; Averick, S.; Page, R. C.; Berberich, J. A.; Konkolewicz, D. The Best of Both Worlds: Active Enzymes by Grafting-to Followed by Grafting-from a Protein. *Chemical Communications* **2015**, *51* (25), 5343–5346. https://doi.org/10.1039/C4CC09287B.
(71) Harrisson, S. The Chain Length Distribution of an Ideal Reversible Deactivation Radical Polymerization. *Polymers (Basel)* **2018**, *10* (8), 887.
(72) Goto, A.; Fukuda, T. Kinetics of Living Radical Polymerization. *Prog Polym Sci* **2004**, *29* (4), 329–385. https://doi.org/https://doi.org/10.1016/j.progpolymsci.2004.01.002.
(73) Kearns, M. M.; Morley, C. N.; Parkatzidis, K.; Whitfield, R.; Sponza, A. D.; Chakma, P.; De Alwis Watuthanthrige, N.; Chiu, M.; Anastasaki, A.; Konkolewicz, D. A General Model for the Ideal Chain Length Distributions of Polymers Made with Reversible Deactivation. *Polym Chem* **2022**, *13* (7), 898–913. https://doi.org/10.1039/D1PY01331A.
(74) Bradford, K. G. E.; Petit, L. M.; Whitfield, R.; Anastasaki, A.; Barner-Kowollik, C.; Konkolewicz, D. Ubiquitous Nature of Rate Retardation in Reversible Addition–Fragmentation Chain Transfer Polymerization. *J Am Chem Soc* **2021**, *143* (42), 17769–17777. https://doi.org/10.1021/jacs.1c08654.
(75) Hutchinson, R. A.; McMinn, J. H.; Paquet, D. A.; Beuermann, S.; Jackson, C. A Pulsed-Laser Study of Penultimate Copolymerization Propagation Kinetics for Methyl Methacrylate/n-Butyl Acrylate. *Ind Eng Chem Res* **1997**, *36* (4), 1103–1113. https://doi.org/10.1021/ie9604031.
(76) Buback, M.; Feldermann, A.; Barner-Kowollik, C.; Lacík, I. Propagation Rate Coefficients of Acrylate−Methacrylate Free-Radical Bulk Copolymerizations. *Macromolecules* **2001**, *34* (16), 5439–5448. https://doi.org/10.1021/ma002231w.
(77) Meyer, V. E.; Lowry, G. G. Integral and Differential Binary Copolymerization Equations. *J Polym Sci A* **1965**, *3* (8), 2843–2851. https://doi.org/https://doi.org/10.1002/pol.1965.100030811.
(78) Van Den Brink, M.; Van Herk, A. M.; German, A. L. Nonlinear Regression by Visualization of the Sum of Residual Space Applied to the Integrated Copolymerization Equation with Errors in All Variables. I. Introduction of the Model, Simulations and Design of Experiments. *J Polym Sci A Polym Chem* **1999**, *37* (20), 3793–3803. https://doi.org/https://doi.org/10.1002/(SICI)1099-0518(19991015)37:20<3793::AID-POLA8>3.0.CO;2-Q.
(79) Moad, G.; Rizzardo, E.; Thang, S. H. Living Radical Polymerization by the RAFT Process. *Aust J Chem* **2005**, *58* (6), 379–410.
(80) McLeary, J. B.; Calitz, F. M.; McKenzie, J. M.; Tonge, M. P.; Sanderson, R. D.; Klumperman, B. Beyond Inhibition: A 1H NMR Investigation of the Early Kinetics of RAFT-Mediated Polymerization with the Same Initiating and Leaving Groups. *Macromolecules* **2004**, *37* (7), 2383–2394. https://doi.org/10.1021/ma035478c.
(81) Beuermann, S.; Harrisson, S.; Hutchinson, R. A.; Junkers, T.; Russell, G. T. Update and Critical Reanalysis of IUPAC Benchmark Propagation Rate Coefficient Data. *Polym Chem* **2022**, *13* (13), 1891–1900. https://doi.org/10.1039/D2PY00147K.
(82) Matyjaszewski, K.; Paik, H.; Zhou, P.; Diamanti, S. J. Determination of Activation and Deactivation Rate Constants of Model Compounds in Atom Transfer Radical

Polymerization. *Macromolecules* **2001**, *34* (15), 5125–5131. https://doi.org/10.1021/ma010185+.
(83) Matyjaszewski, K.; Wang, J.-L.; Grimaud, T.; Shipp, D. A. Controlled/"Living" Atom Transfer Radical Polymerization of Methyl Methacrylate Using Various Initiation Systems. *Macromolecules* **1998**, *31* (5), 1527–1534. https://doi.org/10.1021/ma971298p.
(84) Ando, T.; Kamigaito, M.; Sawamoto, M. Design of Initiators for Living Radical Polymerization of Methyl Methacrylate Mediated by Ruthenium(II) Complex. *Tetrahedron* **1997**, *53* (45), 15445–15457. https://doi.org/https://doi.org/10.1016/S0040-4020(97)00972-1.
(85) Benoit, D.; Chaplinski, V.; Braslau, R.; Hawker, C. J. Development of a Universal Alkoxyamine for "Living" Free Radical Polymerizations. *J Am Chem Soc* **1999**, *121* (16), 3904–3920. https://doi.org/10.1021/ja984013c.
(86) Charleux, B.; Nicolas, J.; Guerret, O. Theoretical Expression of the Average Activation−Deactivation Equilibrium Constant in Controlled/Living Free-Radical Copolymerization Operating via Reversible Termination. Application to a Strongly Improved Control in Nitroxide-Mediated Polymerization of Methyl Methacrylate. *Macromolecules* **2005**, *38* (13), 5485–5492. https://doi.org/10.1021/ma050087e.

For Table of Contents Entry Only

Spontaneous Gradients by ATRP and RAFT: Interchangeable Polymerization Methods?

Kate G. E. Bradford,[a†] Robert D. Gilbert,[a†] M. A. Sachini N. Weerasinghe,[a] Simon Harrisson,[b] Dominik Konkolewicz [a*]

a Department of chemistry and Biochemistry, Miami University, 651 E High St, Oxford, OH, USA
b Laboratoire de Chimie des Polymères Organiques, University of Bordeaux/Bordeaux INP/CNRS UMR5629, Pessac 33600, France
† Authors contributed equally
*Correspondence: d.konkolewicz@miamiOH.edu